New Journal of Physics
The open-access journal for physics

Anharmonicity-induced resonances for ultracold atoms and their detection

J P Kestner[1,2,3] **and L-M Duan**[1]

[1] Department of Physics, University of Michigan, Ann Arbor, MI 48109, USA
[2] Condensed Matter Theory Center, Department of Physics, University of Maryland, College Park, MD 20742, USA
E-mail: jkestner@umd.edu

New Journal of Physics **12** (2010) 053016 (11pp)
Received 19 January 2010
Published 13 May 2010
Online at http://www.njp.org/
doi:10.1088/1367-2630/12/5/053016

Abstract. When two atoms interact in the presence of an anharmonic potential, such as an optical lattice, the center of mass motion cannot be separated from the relative motion. In addition to generating a confinement-induced resonance (or shifting the position of an existing Feshbach resonance), the external potential changes the resonance picture qualitatively by introducing new resonances where molecular excited center of mass states cross the scattering threshold. We demonstrate the existence of these resonances, give their quantitative characterization in an optical superlattice and propose an experimental scheme to detect them through controlled sweeping of the magnetic field.

Contents

[3] Author to whom any correspondence should be addressed.

1. Introduction

In recent years there has been much progress in the study of ultracold atoms in optical lattices, which can cleanly emulate important models in condensed matter, hold promise for quantum computing schemes and offer the prospect of observing many interesting new phenomena [1]. The versatility of this line of research is due in no small part to the control of the atomic interactions afforded by tuning an external magnetic field near a Feshbach resonance [2]. In addition to a magnetic field, a confining potential can be used to tune the scattering length via a Feshbach-type mechanism, typically referred to as a confinement-induced resonance [3] or a trap-induced shape resonance [4], depending on the trap configuration. The trap-induced resonance is basically caused by a shift of the free-space Feshbach resonance point by the confining potential [5]. In an optical lattice, the possibility of decay of atomic pairs due to anharmonic coupling to molecules in an excited center-of-mass (c.m.) state has previously been discussed in [6]. More recently, the possibility of a controlled transfer of an atomic pair to a molecule in an excited c.m. state was discussed in [7]. The anharmonicity of the optical lattice potential has also been recognized as important in obtaining quantitatively accurate predictions for the shift of the free-space Feshbach resonance position, binding energy, etc [8].

In this paper we point out a new effect whereby anharmonic confinement, e.g. from an optical lattice, not only shifts the free-space resonance point, but also induces a series of additional scattering resonances. (A similar effect occurs in mixed dimensions in the absence of anharmonicity [9].) Thus, anharmonicity may give rise not only to population transfer between atom pairs and molecules in different c.m. states, as mentioned to various extents in previous works [6]–[8], but also to a strong modification of the effective atom–atom interaction in the vicinity of the induced scattering resonances. In order to use the optical lattice system as a quantum emulator, it is important to have a full understanding of the dependence of the interaction on the experimental parameters. Even such a basic item as the form of the effective many-body lattice Hamiltonian [11] will be affected in the vicinity of an induced resonance (for a detailed treatment, see [10]). The presence of the additional resonances is then an important consideration for experiment, as well as a novel tool for tuning the interaction utilizing a resonance between atoms and excited c.m. molecules. Measuring population transfer between c.m. states can provide a useful means to look for the resonances. Below, we characterize these anharmonicity-induced resonances in an optical superlattice and propose an experimental scheme to detect their consequences.

To understand the basic mechanism of anharmonicity-induced resonances, let us first compare it to the free-space Feshbach resonance. The free-space Feshbach resonance is caused by coupling between the scattering state of the atomic pair and a highly excited molecular level (the Feshbach molecule), as depicted in figure 1(a). When the energy of the Feshbach molecule, tuned by the external magnetic field, crosses the lowest scattering state, a resonance in the scattering length is signaled [2]. In free space, c.m. and relative motions are decoupled during the atomic scattering, and the c.m. momentum forms a continuum that is not altered by the scattering process.

In the presence of an optical lattice, the continuum spectrum for the atomic and the molecular c.m. motion both split into a series of energy bands. We consider scattering of the atoms in the lowest bands, and only this lowest atomic band is shown in figure 1(b). However, even for this lowest-band atomic scattering, the excited bands for the c.m. motion of the Feshbach molecule still play a significant role due to the anharmonicity of the optical

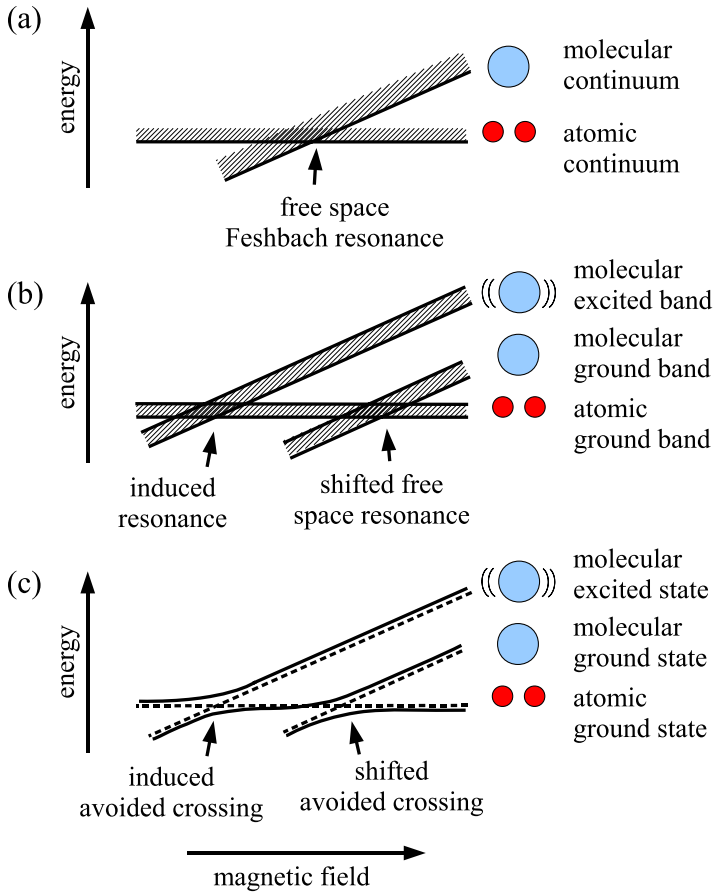

Figure 1. Sketches of the Feshbach type of resonances (a) in free space, (b) in an optical lattice with additional anharmonicity-induced resonances and (c) in a confining potential where the resonances are signaled by the avoided level crossings.

lattice potential. In a harmonic potential, the c.m. motion of two colliding atoms is separated from their relative motion, and thus remains in the lowest band during the collision and does not couple to the Feshbach molecule in the excited bands. However, the anharmonicity of the potential mixes the c.m. and relative motions, and the lowest band scattering state of the atoms is coupled to the Feshbach molecule in *each band*, as depicted in figure 1(b). As one can see from this figure, all the bands for the Feshbach molecule, no matter how excited, eventually cross the atomic scattering threshold as the magnetic field is lowered. This will lead to many resonances for the atomic scattering. In practice, the anharmonic coupling between a Feshbach molecule in the excited band and the atomic pair state in the lowest band will decrease as the band becomes more excited, and the resonances become progressively narrower as the magnetic field is lowered, so only the first few of these resonances are broad enough to be experimentally observable.

In order to quantitatively characterize the anharmonicity-induced resonances, we consider the atoms in an optical superlattice potential. In an optical lattice, direct calculation of the scattering length between two atoms is challenging as one cannot separate the c.m. and

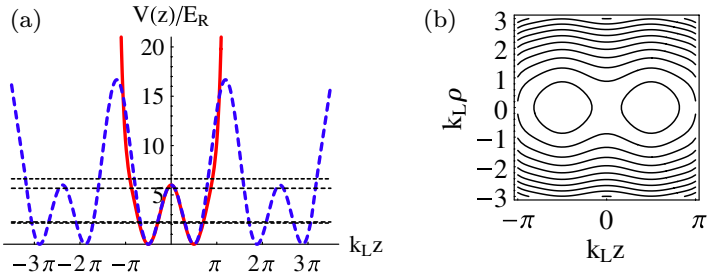

Figure 2. (a) Double-well potential (solid) for a single atom along z and an example of a corresponding superlattice potential (dashed). The horizontal lines are the lowest four single-atom energy levels of the double well. (b) Contour plot of the locally isotropic 3D double well potential.

the relative motion, and solving an equation with all six degrees of freedom is numerically demanding. Instead, here we consider the atoms in a deep superlattice potential [12], which separates the periodic optical lattice into a series of double-well potentials. This has several motivations. Firstly, by adding a confining trap, as illustrated in figure 1(c), the resonance in the continuum scattering spectrum caused by the emergence of a new Feshbach molecular level becomes an avoided level crossing in the discrete spectrum of the trapped atoms. By calculating the width and position of the avoided level crossing, we can approximately characterize the resonance properties for the atomic scattering. Numerically, it is more convenient to deal with the discrete spectrum in a trap that allows the application of the specific calculation techniques presented below. Secondly, the optical superlattice potential has been realized in experiments [12], which allows direct detection of the consequences of the anharmonicity-induced resonances in this kind of trap. We will propose an experimental scheme to test the quantitative predictions from the anharmonicity-induced resonances in a superlattice. Thirdly, the anharmonicity-induced resonances also affect the effective many-body Hamiltonian for strongly interacting atoms in an optical lattice [10, 11]. A natural step to derive such a Hamiltonian is to first consider the effective interaction for atoms in double-well potentials realized with a deep optical superlattice.

2. Methods

We assume that the superlattice potential is along the axial direction z that separates the system into a series of double wells [12]. We consider two atoms of mass m in each double-well potential $V(z)$, approximated by Taylor expanding $V_0 \cos^2(k_L z)$ to 12th order in z. Here V_0 sets the barrier depth and k_L sets the distance between wells and is related to the laser wavevector. Although it is not important for our purposes to exactly fit a particular form of superlattice potential, if one takes a superlattice of the form $\cos^2(kz) + c\sin^2(kz/2)$, then one should choose $k_L = \pi k/(4 \arccos\sqrt{1/2 + c/8})$, as shown in figure 2. (We express energy in units of a 'recoil energy', $E_R = \hbar^2 k_L^2/2m$, and plot the case $V_0 = 6E_R$.) In any case, this potential should be quite sufficient to capture the essential physics in the limit of independent double wells. For ease of calculation, the lattice wells in the transverse directions are approximated by harmonic potentials, with the frequency ω chosen such that the potential is locally isotropic at the bottom of each well.

Due to the harmonicity of the transverse trap, the c.m. motion in the transverse direction separates out and is thus neglected in the rest of the discussion. Also, due to the axial symmetry of the trap, the azimuthal angular dependence of the relative motion separates out. However, along the axis of the double well, the c.m. motion is not separable from the relative motion. The two-atom system then has three relevant coordinates: the relative coordinates z and ρ, along the axial and transverse directions, respectively, and Z, the axial c.m. coordinate. In terms of these coordinates, the external potential with barrier depth V_0 is $V(\rho, z, Z) = V(\rho) + V(z, Z)$, where

$$V(\rho) = V_0 k_{\mathrm{L}}^2 \rho^2/2,$$

$$V(z, Z) = V_0 \sum_{\substack{n=0 \\ \pm}}^{6} \frac{(-4)^n \Gamma(1-2n)}{\Gamma(1-4n)\,\Gamma(1+4n)} k_{\mathrm{L}}^{2n} \left(Z \pm \frac{z}{2}\right)^{2n},$$

with $\Gamma(x)$ being the Euler gamma function, and our summation over signs denotes that for each value of n one must also add the two terms corresponding to the upper and lower signs.

The atoms are interacting via a short-range potential $U(r)$ characterized by its s-wave scattering length a_{s}. The exact form of the interaction is irrelevant as long as its effective range is much smaller than the average interatomic distance and the trap length scale. For a broad s-wave Feshbach resonance, the use of a zero-range pseudopotential is typically justified[4], as has also been confirmed experimentally [14]. Numerically, it is easier to use a finite-range attractive Gaussian interaction $U(r) = -U_0 \exp(-r^2/r_0^2)$, where we typically take $r_0 = 0.05\sqrt{\hbar/m\omega}$. Finite-range effects should be negligible for such small values of r_0, and we have verified this by repeating our calculations with $r_0 = 0.1\sqrt{\hbar/m\omega}$. The free-space scattering length is varied by adjusting the strength of the interaction, U_0. We have used values of U_0 such that the potential supports either zero bound states (for negative scattering length) or one bound state (for positive scattering length). The scattering length goes through resonance when the lowest eigenstate of the interaction potential passes from being unbound to bound.

Adopting units such that $k_{\mathrm{L}} = 1$ and $E_{\mathrm{R}} = \hbar^2 k_{\mathrm{L}}^2/2m = 1$, the Hamiltonian may be written as

$$H = -\frac{2}{\rho}\frac{\partial}{\partial\rho}\rho\frac{\partial}{\partial\rho} - 2\frac{\partial^2}{\partial z^2} - \frac{1}{2}\frac{\partial}{\partial Z^2} + 2\frac{m_\ell^2}{\rho^2} + V(\rho, z, Z) - U_0\, \mathrm{e}^{-(z^2+\rho^2)/r_0^2}, \tag{1}$$

where m_ℓ is the relative angular momentum, which is a good quantum number due to axial symmetry. In the following, we will consider only $m_\ell = 0$, since in the limit as r_0 goes to zero, the interaction does not affect states with $m_\ell \neq 0$.

We find the low-lying states of the system using a stochastic variational method [15]. In this approach, the variational wavefunction takes the form

$$\Psi(\rho, z, Z) = \sum_i^N \alpha_i \exp\left(-\rho^2/a_i^2 - z^2/b_i^2 - Z^2/c_i^2\right), \tag{2}$$

where α is a linear variational parameter, $\{a, b, c\}$ are nonlinear variational parameters that define the basis elements and N is the size of the basis set. The nonlinear parameters are selected from stochastically generated pools of candidates to minimize the variational energy

[4] See e.g. [13] for a comparison of zero-range pseudopotential results versus realistic numerical calculations in a harmonic trap.

$\langle\Psi|H|\Psi\rangle/\langle\Psi|\Psi\rangle$. The basic algorithm is as follows: starting with a set of $N-1$ basis states,

1. a pool of (in our calculations) 25 new basis states is randomly generated, each defined by a given value of $\{a_i, b_i, c_i\}$;
2. for each of the 25 possible N-dimensional basis sets formed by adding one basis from the candidate pool, the energy is minimized with respect to α; and
3. the new basis set that yields the lowest energy is kept and the previous steps are repeated until the basis size, N, increases to the desired number.

Once every few iterations, the existing basis set is optimized by the following refining process: starting with a set of N basis states and $n = 1$,

(a) a pool of 25 replacement basis states is randomly generated, each defined by a given value of $\{a_n, b_n, c_n\}$;
(b) for each of the 25 possible N-dimensional basis sets formed by replacing the nth old basis state with a new one from the candidate pool, the energy is minimized with respect to α;
(c) if the lowest of these 25 energies is lower than the current variational energy, the nth old basis state is replaced by the new optimal one and the previous steps are repeated for $n = 1, \ldots, N$.

We typically achieve fairly good convergence for $N \sim 300$. Although in principle the nonlinear basis optimization must be performed for each value of a_s, actually the basis set does not change too much as one sweeps across resonance except to include narrower and narrower Gaussians for positive a_s where deeply bound molecules form. Apart from deeply bound states, the change in the wavefunction is mainly due to changing the expansion coefficients, α. To save computational time, then, we performed the nonlinear basis optimization for four different values of a_s ranging from positive to negative, joined the four optimized basis sets, and simply minimized the energy with respect to α using the resultant basis set of about 1200 elements for all values of a_s.

3. Results

3.1. Spectrum

In figure 3, we show the energy spectrum of two particles interacting near a free-space Feshbach resonance ($1/k_L a_s = 0$) in the double-well potential. For clarity, we have omitted the levels corresponding to wavefunctions of odd parity in z or Z (which have no contribution to the anharmonicity-induced resonances) and plunging levels for $-1/k_L a_s < -10$. We have explicitly labeled the lowest few states for later reference. To understand figure 3, it is useful to use the language of the two-channel picture of atom pairs coupled to molecules, as in figure 1. Without coupling, there are plunging molecular levels crossing flat (i.e. noninteracting) atom pair levels, as depicted by the dashed lines in figure 1(c). When one turns on atom–molecule coupling only between molecules and atoms with the same c.m. motion, the crossings between the lowest plunging molecular level and the flat atomic levels become avoided crossings and the spectrum is similar to the well-known results for a harmonic trap [16]. The atoms and the lowest c.m. molecules hybridize, such that as the inverse scattering length is adiabatically swept from negative values to positive values, the lowest atomic level evolves into the lowest molecular

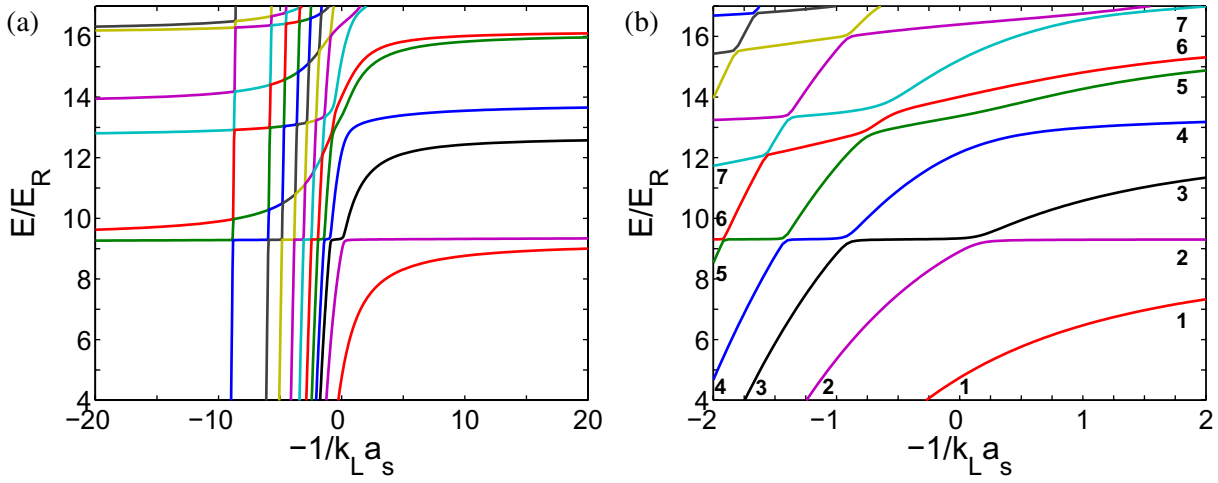

Figure 3. (a) Spectrum of two strongly interacting atoms in a three-dimensional double-well potential with $V_0 = 6E_R$. Only the first few plunging levels are shown. (b) Close-up of the strongly interacting region. The first few states are explicitly labeled for reference.

level and a given excited atomic level will evolve into the next lowest atomic level, sweeping out a sigmoidal path. (For a double well, the lowest two atomic levels form a closely spaced doublet; hence in the presence of coupling, the lowest sigmoidal level is essentially flat, as in figure 3(a). Higher-lying doublets behave likewise.)

If we take anharmonicity into account by also allowing coupling between the atoms and excited c.m. molecules, the crossings between the higher plunging molecular levels and the flat atomic levels also become narrow avoided crossings. These signal the presence of a rich set of induced resonances. The resonances are weak relative to the free-space resonance and become progressively weaker away from $1/k_L a_s = 0$, so that only the first few are observable. Diabatically, then, figure 3 displays three kinds of curves: plunging levels corresponding to tightly bound molecules, flat levels corresponding to atoms in separate wells and sigmoidal levels corresponding to atoms with overlapping wavefunctions such that they interact while maintaining a nonvanishing pair size unlike the tightly bound molecules. Note that the many plunging molecular levels, of which we have shown only the first few, are associated with the various states of the trap, as sketched in figure 1(c). They are *motionally* excited c.m. states, not internally excited states of the interaction potential. Also note that for an optical lattice, one will obtain a similar spectrum except that the discrete levels of the double well shown in figure 3 (analogous to figure 1(c)) will broaden into bands (analogous to figure 1(b)).

3.2. Avoided crossing data

To characterize the anharmonicity-induced resonance, we estimate the time required to adiabatically sweep across the avoided level crossing, transferring population between atomic and molecular states. In the Landau–Zener approximation [17], the probability of an adiabatic transfer at sweep rate $\partial B/\partial t = v$ is $P_{ad} = 1 - \exp(-v_{LZ}/v)$, where the Landau–Zener parameter $v_{LZ} = \pi\Delta^2/2\hbar|\partial\Delta/\partial B|$; Δ is the minimum energy gap between the two levels in question, and $\partial\Delta/\partial B$ is the rate at which the energy gap changes with the magnetic field away from the avoided crossing. The energy splitting Δ for the avoided level crossing should be proportional

Table 1. Anharmonicity-induced avoided level crossing data for ^{6}Li (^{40}K) atoms at $V_0 = 6E_R$. These are the avoided crossings near $E = 9.3E_R$ shown in figure 3.

	$-1/k_L a_s$	Δ/h (kHz)	t_{min} (μs)	v_{LZ} (G s^{-1})
^{6}Li	0.2	8	40	2×10^6
	−0.9	8	70	3×10^5
	−1.4	5	100	6×10^4
	−1.9	1	200	2×10^3
	−2.5	0.3	1×10^3	40
^{40}K	0.2	1	600	800
	−0.9	1	600	400
	−1.4	0.8	1×10^3	100
	−1.9	0.2	2×10^3	6
	−2.5	0.05	1×10^4	0.1

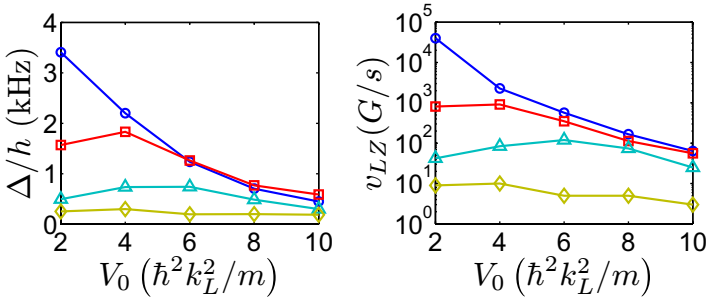

Figure 4. (a) Energy gap and (b) Landau–Zener parameter for the first four avoided crossings versus well depth for ^{40}K atoms. From the top to the bottom, the curves correspond to the avoided crossings shown in figure 3(b) at $E = 9.3E_R$ and $-1/k_L a_s = 0.2, -0.9, -1.4$ and -1.9, respectively.

to the width of the corresponding anharmonicity-induced resonance in a periodic optical lattice. This parameter Δ is listed in table 1 for the various avoided crossings between excited molecular states and the lowest atomic level (near $E = 9.3E_R$) for ^{6}Li or ^{40}K atoms. The numbers quoted are of course only a rough guide to what may be expected in experiment and are not intended to be quantitatively precise—recall that the double-well potential we have taken is only an approximation to whatever form the actual potential may take. To connect our results to experiment, we assume that the scattering length is related to the magnetic field via the usual relation $a_s = a_{bg}[1 - W/(B - B_0)]$, where a_{bg} is the background scattering length, W is the resonance width and B_0 is the resonance point. We take $k_L \sim 2\pi/1\ \mu$m and consider ^{6}Li (^{40}K) near the free-space Feshbach resonance at 834 G [18] (202 G [19]). In table 1, we have also listed an estimate of the minimum time, t_{min}, required to ramp across the avoided crossing at the critical rate, v_{LZ}. If the time available in the experiment to perform the ramp is of the order of a few milliseconds, appreciable adiabatic transfer is feasible across the first five (four) avoided crossings for ^{6}Li (^{40}K) atoms.

We have performed the same kind of calculations for several lattice depths. In figure 4, we show how the energy splitting Δ and the Landau–Zener parameter v_{LZ} for the first few

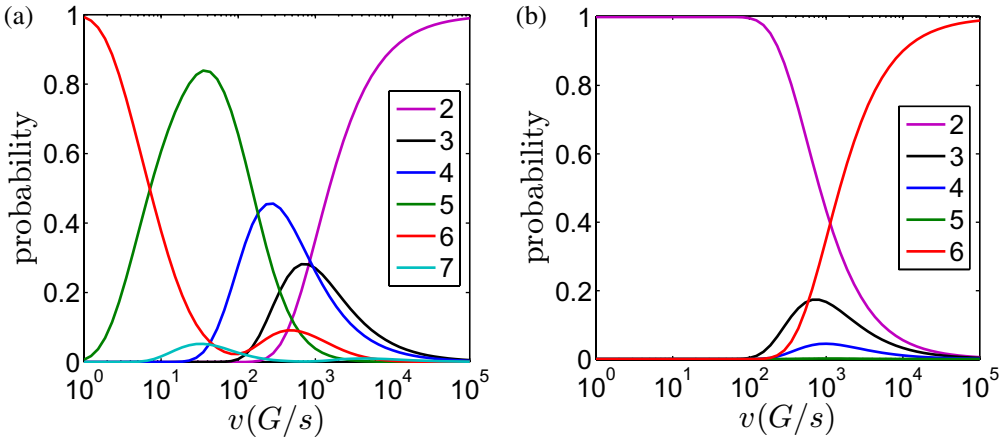

Figure 5. Final population distribution versus ramp speed of the magnetic field (a) from state 6 at $-1/k_{\mathrm{L}}a_{\mathrm{s}} = -2$ to states 2–7 at $-1/k_{\mathrm{L}}a_{\mathrm{s}} = 2$ or (b) from state 2 at $-1/k_{\mathrm{L}}a_{\mathrm{s}} = 2$ to states 2–6 at $-1/k_{\mathrm{L}}a_{\mathrm{s}} = -2$. Both plots are for ^{40}K atoms with $V_0 = 6E_{\mathrm{R}}$. In (b), the probability of sweeping into state 5 at $-1/k_{\mathrm{L}}a_{\mathrm{s}} = -2$ is essentially zero at any ramp speed.

resonances listed in table 1 change as V_0 is varied for ^{40}K. Generally, the energy splitting for the avoided level crossing decreases for deeper wells, as one would expect due to suppression of the anharmonicity in a deep lattice (the harmonic approximation becomes better for a deep lattice well). For very shallow wells, however the potential apparently cannot couple the higher c.m. states of Feshbach molecules with the lowest atomic state as efficiently, and the energy splitting Δ actually increases with lattice depth at first for small V_0. However, for very excited c.m. states (corresponding, e.g., to the bottom curve in figure 4), the weak coupling with the lowest atomic state evidently does not depend as strongly on the lattice depth. As the potential wells are deepened, the resonance positions shift slightly to lower magnetic fields.

3.3. Detection

To experimentally detect the avoided level crossings associated with the anharmonicity-induced resonances, one can take the following steps. Firstly, one loads the optical superlattice in the weakly interacting region with two atoms in each double well [12, 20]. The inter-well barrier is kept high so that one has a Mott state with one atom per well. Secondly, one ramps the system to the strongly interacting region with $-1/k_{\mathrm{L}}a_{\mathrm{s}} = \pm 2$ and then quickly lowers the inter-well barrier to the desired value (with $V_0 = 6E_{\mathrm{R}}$ in our example), leaving the atoms still in the Mott state (at energy $E \simeq 9.3E_{\mathrm{R}}$ in figure 3) at this moment. The magnetic field is then adiabatically ramped across the anharmonicity-induced resonances, and one detects the resulting population distribution after the ramp. To perform the detection, the inter-well barrier is quickly turned back up with a time scale that is fast compared to the inter-well dynamics, but still slow compared to the lattice band gap (or the single-well energy gap). This freezes the system evolution again before the magnetic field is ramped to the deep BEC side ($-1/k_{\mathrm{L}}a_{\mathrm{s}} \ll -1$), separating the molecular levels from the atomic levels. One can then selectively take absorption images of either the atoms or the molecules [21], and measure their distribution over different bands through a band-mapping procedure [12]. The presence of the anharmonicity-induced level crossings can then be inferred from the final population distribution.

As an example, in figure 5(a), we show the Landau–Zener calculation results for ^{40}K atoms at $V_0 = 6E_R$ (b) swept from $-1/k_L a_s = -2$ to $-1/k_L a_s = 2$ with the atoms starting in state 6 labeled in figure 3(b). For fast sweeps, the atoms change states diabatically to remain at about the same energy, as would be expected in the absence of anharmonicity. In the adiabatic limit, all the atoms remain in state 6, which corresponds at $-1/k_L a_s = 2$ to atoms in an excited state. At intermediate speeds, several atomic states become populated. A sweep in the opposite direction, from $-1/k_L a_s = 2$ to -2, starting with atoms in state 2, is shown in figure 5(b). When sweeping in this direction, population can be transferred to tightly bound molecules in several excited c.m. states (states 2–5 at $-1/k_L a_s = -2$) as well as diabatically to atoms near the initial energy (state 6).

4. Summary

We predict the existence of several Feshbach-type resonances induced by the anharmonicity of the optical lattice, which couples the Feshbach molecules in the excited bands and the atomic states in the lowest band. We have characterized the corresponding set of avoided level crossings in the calculated spectrum of two atoms interacting in a superlattice potential, and proposed an experimental scheme to observe these avoided crossings through slow sweeps of the magnetic field. The anharmonicity-induced resonances may prove to be a useful tool for the manipulation of interaction between ultracold atoms in optical lattice potentials.

Acknowledgment

This work was supported by the AFOSR through MURI, the DARPA and the IARPA.

References

[1] Bloch I 2005 *Nat. Phys.* **1** 23
Jaksch D and Zoller P 2005 *Ann. Phys., NY* **315** 52
Bloch I, Dalibard J and Zwerger W 2008 *Rev. Mod. Phys.* **80** 885
[2] Timmermans E *et al* 1999 *Phys. Rep.* **315** 199
Duine R A and Stoof H T C 2004 *Phys. Rep.* **396** 115
Chin C, Grimm R, Julienne P and Tiesinga E 2008 arXiv:0812.1496v1
[3] Olshanii M 1998 *Phys. Rev. Lett.* **81** 938
Bergeman T, Moore M G and Olshanii M 2003 *Phys. Rev. Lett.* **91** 163201
Fedichev P O, Bijlsma M J and Zoller P 2004 *Phys. Rev. Lett.* **92** 080401
[4] Stock R, Deutsch I H and Bolda E L 2003 *Phys. Rev. Lett.* **91** 183201
Krych M and Idziaszek Z 2009 *Phys. Rev.* A **80** 022710
[5] Kohl M *et al* 2005 *Phys. Rev. Lett.* **94** 080403
[6] Bolda E L, Tiesinga E and Julienne P S 2005 *Phys. Rev.* A **71** 033404
[7] Mentink J and Kokkelmans S 2009 *Phys. Rev.* A **79** 032709
[8] Deuretzbacher F *et al* 2008 *Phys. Rev.* A **77** 032726
Grishkevich S and Saenz A 2009 *Phys. Rev.* A **80** 013403
Schneider P-I, Grishkevich S and Saenz A 2009 *Phys. Rev.* A **80** 013404
[9] Nishida Y and Tan S 2008 *Phys. Rev. Lett.* **101** 170401
[10] Kestner J P and Duan L-M 2010 *Phys. Rev.* A, to be published, preprint arXiv:0912.1640

[11] Duan L-M 2005 *Phys. Rev. Lett.* **95** 243202
Duan L-M 2008 *Europhys. Lett.* **81** 20001
[12] Folling S *et al* 2007 *Nature* **448** 1029
Anderlini M *et al* 2007 *Nature* **448** 452
Trotzky S *et al* 2008 *Science* **319** 295
[13] Chen Y and Gao B 2007 *Phys. Rev.* A **75** 053601
[14] Stoferle T *et al* 2006 *Phys. Rev. Lett.* **96** 030401
[15] Suzuki Y and Varga K 1998 *Stochastic Variational Approach to Quantum-Mechanical Few-Body Problems* (Berlin: Springer)
von Stecher J and Greene C H 2007 *Phys. Rev. Lett.* **99** 090402
[16] Busch T, Englert B-G, Rzazewski K and Wilkens M 1998 *Found. Phys.* **28** 549
[17] Zener C 1932 *Proc. R. Soc.* A **137** 696
[18] Bartenstein M *et al* 2005 *Phys. Rev. Lett.* **94** 103201
[19] Regal C A, Greiner M and Jin D S 2004 *Phys. Rev. Lett.* **92** 040403
[20] Goodman T and Duan L-M 2009 *Phys. Rev.* A **79** 023617
[21] Regal C A *et al* 2003 *Nature* **424** 47